galaxies

MDPI

Article

Modeling Polarized Emission from Black Hole Jets: Application to M87 Core Jet

Monika Mościbrodzka

Department of Astrophysics, The Institute for Mathematics, Astrophysics and Particle Physics, Radboud University, P.O. Box 9010, 6500 GL Nijmegen, The Netherlands; m.moscibrodzka@astro.ru.nl

Academic Editors: Emmanouil Angelakis and Jose L. Gómez
Received: 18 August 2017; Accepted: 13 September 2017; Published: 19 September 2017

Abstract: We combine three-dimensional general-relativistic numerical models of hot, magnetized Advection Dominated Accretion Flows around a supermassive black hole and the corresponding outflows from them with a general relativistic *polarized* radiative transfer model to produce synthetic radio images and spectra of jet outflows. We apply the model to the underluminous core of M87 galaxy. The assumptions and results of the calculations are discussed in context of millimeter observations of the M87 jet launching zone. Our ab initio polarized emission and rotation measure models allow us to address the constrains on the mass accretion rate onto the M87 supermassive black hole.

Keywords: black holes; jets; polarized emission; GRMHD simulations

1. Introduction

AGN jets are believed to be powered by the accretion of material from their host galaxy onto a supermassive black hole [1]. The long standing question is: What are the roles of the accretion disk, magnetic fields and the black hole spin in the formation of these relativistic flows?

We investigate the physical conditions in the jet launching zone in global three-dimensional, general relativistic magnetohydrodynamical (3-D GRMHD) simulations. The numerical models follow the dynamics of fully ionized plasma and magnetic fields down to the black hole event horizon. Similar simulations have been performed by several groups [2–9]. A recent breakthrough in GRMHD models of black hole accretion and jets comes from modeling the radiation from plasma near the black hole [10–12]. Until recently, the least understood part of these models was a proper treatment of radiating electrons. Finally, however, this issue has been addressed [13–19]. With new and more detailed observations, we are beginning to directly compare the numerical simulations of accretion flows to real astronomical systems such as Galactic center Sgr A* and the core of M87 galaxy [20].

2. GRMHD Models of Jets

Here, we describe a fiducial 3-D GRMHD model of accretion disk with a jet. Example simulations are carried out with the HARM-3D code [4,6] by [21]. The code solves ideal-MHD equations in a fixed Kerr metric. These models do not include radiative losses; hence, they are applicable to sources that are rather underluminous ($L/L_{\rm Edd} < 10^{-7}$). Models with radiative looses taken into account selfconsistently shall be explored in the future [22,23].

At $t = 0$, the plasma is confined to a geometrically-thick donut-shaped torus. The plasma density distribution, internal energy and velocity are computed using an analytical torus model presented in [24]. The inner edge of the torus is $r_{\rm in} = 12GM/c^2$, and the position of the plasma pressure maximum is $r_{\rm max} = 24GM/c^2$. The size of the computational domain extends to $r_{\rm out} = 240GM/c^2$. We follow standard procedures and seed the initial plasma with a sub-thermal magnetic field ($\beta = P_{\rm gas}/P_{\rm mag} = 10 - 100$), with its geometry aligned with the iso-density surfaces of the torus

(the so-called single loop scenario). The free parameter is the black hole spin chosen to be $a_* = cJ/GM^2 = 0.9375$.

Jets appear almost naturally in our simulations. The rotational energy of the black hole and accretion disk is extracted through a combination of the well-known Blandford-Znajek and Blandford-Payne mechanisms [25,26]. Typically, the models described here are called SANE in the current jargon, which stand for Standard And Normal Evolution, having low-power jets. Other solutions with stronger magnetic fields and more powerful jets are equally possible [27,28].

3. Electron Treatment and Modeling Polarized Emission from GRMHD Jets

The GRMHD simulations provide only the fluid pressure, which is dominated by the protons. In a perfect fluid, the pressure in a grid zone gives a proton temperature. For underluminous accretion flows (in Sgr A* and M87), protons and electrons are not necessarily well coupled. We have to assume an electron temperature as they are not self-consistently computed in the considered GRMHD simulations, but they are essential in calculating the synchrotron emission.

Inspired by early models for radio cores in quasars [1] and the Solar corona plasma models [19,29,30], we have developed a simple parametric description for electron thermodynamics in the simulation of accretion flows. In combination with radiative transfer model, this finally makes our numerical simulations of accretion flows resemble observations of underluminous accreting black holes [13,14,16,18,31].

Our parametric model for electrons assumes a thermal relativistic (Maxwell-Jüttner) distribution function. The electron temperatures, T_e, are computed assuming that the proton-to-electron coupling depends on plasma magnetization [14,16,18]:

$$\frac{T_p}{T_e} = R_{\rm low}\frac{1}{1+\beta^2} + R_{\rm high}\frac{\beta^2}{1+\beta^2}, \quad (1)$$

where $\beta = P_{\rm gas}/P_{\rm mag}$ is ratio of the gas pressure to magnetic field pressure $P_{\rm mag} = B^2/2$ (where B and hence $P_{\rm mag}$ and $P_{\rm gas}$ are in the HARM code units). $R_{\rm low}$ and $R_{\rm high}$ are two free parameters. In a strongly magnetized plasma, $\beta \ll 1$ and $T_p/T_e \to R_{\rm low}$. In a weakly magnetized plasma, $\beta \gg 1$ and so $T_p/T_e \to R_{\rm high}$. We set $R_{\rm low} = 1$ and $R_{\rm high} = 100$ so that the electrons are always cooler in the disk but hotter towards the jet, making the jet more visible.

A ray-tracing approach is used to construct mock observations of GRMHD simulations. The radiative transfer equations through changing plasma conditions for a single photon frequency ν are integrated along null-geodesic paths. This approach is valid only if the plasma index of refraction is one. The ray-tracing radiative transfer methods can be also used only if the photon frequency is much larger than the plasma cyclotron frequency, and is larger than the plasma frequency, ν_p (i.e., $\nu \gg \nu_c = 2.8\times10^6 B$, $\nu \gg \nu_p = 8980\, n_e^{1/2}$ Hz). In our GRMHD models, typically, $n_e = 10^2 - 10^7 {\rm cm}^{-3}$ and $B = 0.1 - 100$ Gauss, so our plasma $\nu_c = 2.8\times10^{-4} - 0.28$ GHz and $\nu_p = 8.9\times10^{-5} - 0.028$ GHz. Here we model emission at $\nu = 43 - 230$ GHz (λ=7 – 1mm), so the approach is valid.

Several existing numerical codes can generate polarized images of radiative plasma near black holes (e.g. [32,33]). In this proceeding we present results based on our new radiative transfer code ipole [34]. The unique feature of our scheme is that it is fully covariant, and so it is suitable for parallel transport of polarized light rays in arbitrary spacetimes and coordinates. We also use the analytical solution to evolve Stokes vector that guarantees stability of the radiative transfer solutions regardless of physical conditions in the plasma. Our model is therefore applicable to plasma with high optical and Faraday depth, which are likely common in jets embedded in cooler accretion flows. We have demonstrated that our integration scheme is stable and accurate; it reproduces known analytic radiative transfer solutions in our method paper [34].

4. Simulated Emission from M87 Core Jet

Figure 1 displays the apperance of the simulations scaled to M87 central supermassive black hole with its mass $M_{\rm BH} = 6.2 \times 10^9 {\rm M}_\odot$. We show the model in polarized light at three different wavelengths (λ= 7.0, 3.5 and 1.3 mm) at which the source is often observed [35–37]. The 1.3 mm synthetic images have been published in [16,18]. Here, we have extended our previous results to the other wavelengths.

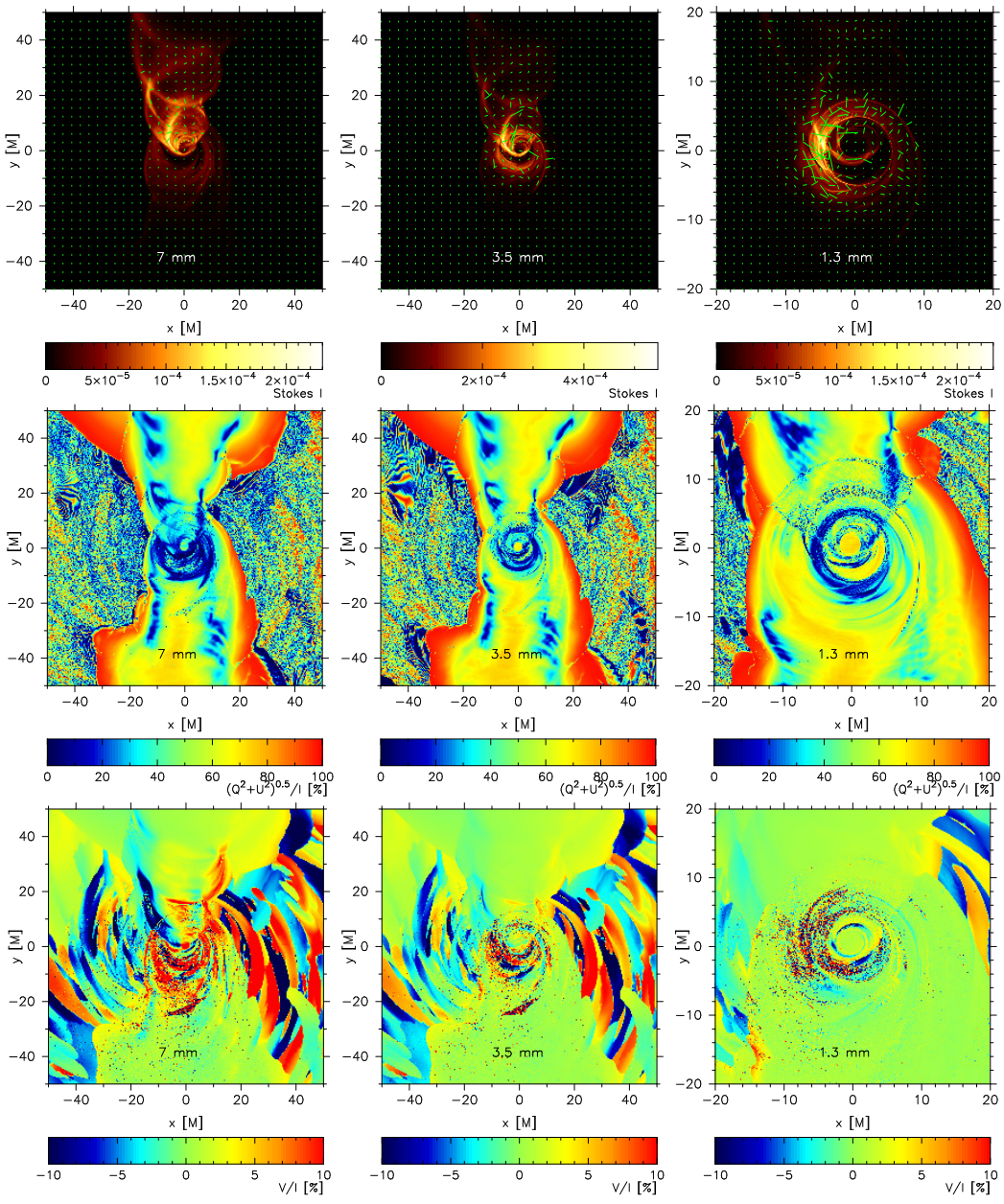

Figure 1. From left to right, the panels show the appearance of the GRMHD model of a relativistic jet in polarized light at three wavelengths at which the M87 core jet is typically observed. The viewing angle is $i = 20^\circ$ off the black hole spin axis, and the polarized radiative transfer calculations are carried out within r < 50 GM/c^2 as beyond that regions the models are not relaxed. Notice that the rightmost panels display the image of the model just near the black hole event horizon. Top panels: the intensity of radiation (the same total intensity maps are published in [16]) overplotted with polarization ticks. The length of each tick is proportional to the local $\sqrt{Q^2 + U^2}$. Middle panels: the corresponding maps of the linear polarization degree. Bottom panels: maps of the circular polarization degree. The 1.3 mm image in the topright panel has been published in [16,18].

Synchrotron emission is intrinsically highly polarized. For ultra-relativistic thermal electrons, the linear polarization fraction measured locally can reach nearly 100% [38]. In our images, the brightest regions are typically linearly depolarized and polarization ticks are scrambled. Both effects are due to strong Faraday effects. We found that the Faraday optical depth in our models is $\tau_F \gg 1$. This suggests that even though the Advection Dominated Aaccretion Flows (ADAF)-type accretion flows are optically thin, they can still be Faraday thick (for details see [18]). Interestingly, in our models we also observe non-zero circular polarization. The theoretical synchrotron maps should be convolved with instrumental effects before direct comparison to the Very Long Baseline Interferometric images on M87 core jet [37,39].

A direct application of our polarized images is to model an observed rotation measure (RM) and provide a model dependent constrain on the mass accretion/outflow rate of the M87 black hole. There are a few observations of RM near supermassive black holes [40–44], including the core of M87 with $|\mathrm{RM}| < 7.5 \times 10^5\,\mathrm{rad\,m^{-2}}$ [36]. All these RM are measured at millimeter wavelengths with non-VLBI observations thus the sources are not resolved. The observed RM was then used to constrain the mass accretion rate onto the central object. The usual procedure to interpret the observed RM is to integrate

$$\mathrm{RM} = 10^4 \frac{e^3}{2\pi m_e^2 c^4} \int f_{\mathrm{rel}} n_e B_{||} dl \quad [\mathrm{rad\,m^{-2}}] \tag{2}$$

in the radial direction with a power-law profiles for n_e and B (usually from equipartition condition) from a semi-analytical ADAF model (e.g., [45]). In Equation (2), all physical constants are in c.g.s. units while 10^4 factor converts RM from c.g.s. to SI units. Notice also that Equation (2) assumes that the polarized source behind is an 'external' Faraday screen. The accretion rate onto the black hole is then provided by the ADAF model [46]. In Sgr A*, the rotation measure of $-5.6 \pm 0.7 \times 10^5\,\mathrm{rad\,m^{-2}}$ was used to estimate $\dot{M} = 5 \times 10^{-9} - 2 \times 10^{-7}\,\mathrm{M_\odot yr^{-1}}$ where the lower and upper limits correspond to different slopes of the electron density radial profiles, which depend on the presence and properties of an outflow assumed to be produced by accretion process [40,41,46]. Following the same procedure, the upper limit for RM in the M87 core led to an accretion rate constraint of $\dot{M} < 9 \times 10^{-4}\,\mathrm{M_\odot yr^{-1}}$ [36,47].

Our radiative transfer model allow us to directly calculate the change of polarization angle $\chi \equiv arg(Q + iU)/2$ as a function of wavelength and compute the model $\mathrm{RM} = (\chi_{\lambda_1} - \chi_{\lambda_2})/(\lambda_1^2 - \lambda_2^2)$ without using approximate formulas, such as Equation (2). Contrary to many previous RM modelings, in the current RM model all relativistic effects will be included; the observer viewing angle effects and the magnetic field geometry are naturally taken into account; the mass accretion rate onto the black hole is self-consistently calculated within the GRMHD simulation. Based on radiative transfer calculations at 220–230 GHz our model predict observed $\mathrm{RM}=6 \times 10^5\mathrm{radm^{-2}}$ which is consisitent with observations. Interestingly, our model accretion rate is $\dot{M} = 9 \times 10^{-3}\mathrm{M_\odot yr^{-1}}$, which is an order of magnitude larger than previous estimates for this source.

5. Discussion

The polarized emission models demonstrate that observed changes in total polarization angle should be interpreted more carefully as they could be model dependent. The previous constraints of accretion rate onto underluminous black holes assumed that the polarized emission is produced near the black hole, and is Faraday rotated in the extended accretion flow. In Sgr A*, the compact emission region [48], observed scaling of $\chi \sim \lambda^2$, and $\simeq 10$ per cent RM variability [41] support this scenario and motivate the use of Equation (2). In the M87 jet models the accretion flow is simultaneously the source of synchrotron radiation and the Faraday screen. Consequently, the polarization plane position angle χ does not have to be constant with λ^2 (as if it were the polarized source behind an 'external' Faraday screen) and Equation (2) may not be directly applicable. This is because the accretion flow has complex structure where the self-absorption and depolarization of radiation take place. Additionally, especially in M87, the emission near the black hole may not be produced by an accretion flow such as ADAF, but, e.g., by a jet; hence, the existing measurements would be probing the plasma flowing out

from the central region (also because of our viewing angle of the jet). In our models, the polarized flux is produced and Faraday rotated in the forward jet. As a consequence the accretion rate onto the black hole is allowed to be higher.

Acknowledgments: Author acknowledges support from the ERC Synergy Grant "BlackHoleCam-Imaging the Event Horizon of Black Holes" (Grant 610058). This publication has received funding from the European Union's Horizon 2020 research and innovation programme under grant agreement No 730562 [RadioNet]. Author acknowledges H. Shiokawa for providing the 3D GRMHD simulations data.

Conflicts of Interest: The authors declare no conflict of interest.

References

1. Blandford, R.D.; Königl, A. Relativistic jets as compact radio sources. *Astrophys. J.* **1979**, *232*, 34–48.
2. Hawley, J.F.; Balbus, S.A.; Stone, J.M. A Magnetohydrodynamic Nonradiative Accretion Flow in Three Dimensions. *Astrophys. J. Lett.* **2001**, *554*, L49–L52.
3. De Villiers, J.P.; Hawley, J.F. A Numerical Method for General Relativistic Magnetohydrodynamics. *Astrophys. J.* **2003**, *589*, 458–480.
4. Gammie, C.F.; McKinney, J.C.; Tóth, G. HARM: A Numerical Scheme for General Relativistic Magnetohydrodynamics. *Astrophys. J.* **2003**, *589*, 444–457.
5. Anninos, P.; Fragile, P.C.; Salmonson, J.D. Cosmos++: Relativistic Magnetohydrodynamics on Unstructured Grids with Local Adaptive Refinement. *Astrophys. J.* **2005**, *635*, 723–740.
6. Noble, S.C.; Gammie, C.F.; McKinney, J.C.; Del Zanna, L. Primitive Variable Solvers for Conservative General Relativistic Magnetohydrodynamics. *Astrophys. J.* **2006**, *641*, 626–637.
7. McKinney, J.C. General relativistic force-free electrodynamics: A new code and applications to black hole magnetospheres. *Mon. Not. R. Astron. Soc.* **2006**, *367*, 1797–1807.
8. White, C.J.; Stone, J.M.; Gammie, C.F. An Extension of the Athena++ Code Framework for GRMHD Based on Advanced Riemann Solvers and Staggered-mesh Constrained Transport. *Astrophys. J. Suppl. Ser.* **2016**, *225*, 22.
9. Porth, O.; Olivares, H.; Mizuno, Y.; Younsi, Z.; Rezzolla, L.; Mościbrodzka, M.; Falcke, H.; Kramer, M. The Black Hole Accretion Code. *ArXiv* **2016**, arXiv:gr-qc/1611.09720.
10. Mościbrodzka, M.; Gammie, C.F.; Dolence, J.C.; Shiokawa, H.; Leung, P.K. Radiative Models of SGR A* from GRMHD Simulations. *Astrophys. J.* **2009**, *706*, 497–507.
11. Dexter, J.; Agol, E.; Fragile, P.C.; McKinney, J.C. The Submillimeter Bump in Sgr A* from Relativistic MHD Simulations. *Astrophys. J.* **2010**, *717*, 1092–1104.
12. Shcherbakov, R.V.; Penna, R.F.; McKinney, J.C. Sagittarius A* Accretion Flow and Black Hole Parameters from Gene ral Relativistic Dynamical and Polarized Radiative Modeling. *Astrophys. J.* **2012**, *755*, 133.
13. Mościbrodzka, M.; Falcke, H. Coupled jet-disk model for Sagittarius A*: Explaining the flat-spectrum radio core with GRMHD simulations of jets. *Astron. Astrophys.* **2013**, *559*, L3–L7.
14. Mościbrodzka, M.; Falcke, H.; Shiokawa, H.; Gammie, C.F. Observational appearance of inefficient accretion flows and jets in 3D GRMHD simulations: Application to Sagittarius A*. *Astron. Astrophys.* **2014**, *570*, A7–A16.
15. Chan, C.K.; Psaltis, D.; Özel, F.; Narayan, R.; Saḍowski, A. The Power of Imaging: Constraining the Plasma Properties of GRMHD Simulations using EHT Observations of Sgr A*. *Astrophys. J.* **2015**, *799*, doi:10.1088/0004-637X/799/1/1.
16. Mościbrodzka, M.; Falcke, H.; Shiokawa, H. General relativistic magnetohydrodynamical simulations of the jet in M 87. *Astron. Astrophys.* **2016**, *586*, A38.
17. Gold, R.; McKinney, J.C.; Johnson, M.D.; Doelema n, S.S. Probing the magnetic field structure in Sgr A* on Black Hole Hori zon Scales with Polarized Radiative Transfer Simulations. *ArXiv* **2016**, arXiv:1601.05550.
18. Mościbrodzka, M.; Dexter, J.; Davelaar, J.; Falcke, H. Faraday rotation in GRMHD simulations of the jet launching zone of M87. *Mon. Not. R. Astron. Soc.* **2017**, *468*, 2214–2221.
19. Ressler, S.M.; Tchekhovskoy, A.; Quataert, E.; Gammie, C.F. The disc-jet symbiosis emerges: Modelling the emission of Sagittarius A* with electron thermodynamics. *Mon. Not. R. Astron. Soc.* **2017**, *467*, 3604–3619.

20. Goddi, C.; Falcke, H.; Kramer, M.; Rezzolla, L.; Brinkerink, C.; Bronzwaer, T.; Deane, R.; De Laurentis, M.; Desvignes, G.; Davelaar, J.R.J.; et al. BlackHoleCam: Fundamental physics of the Galactic center. *ArXiv* **2016**, arXiv:1606.08879.
21. Shiokawa, H. General-Relativistic Magnetohydrodynamics Simulations of Black ho le Accretion Disks: Dynamics and Radiative Properties. Ph.D. Thesis, University of Illinois at Urbana-Champaign, Champaign, IL, USA, 2013.
22. Ryan, B.R.; Dolence, J.C.; Gammie, C.F. bhlight: General Relativistic Radiation Magnetohydrodynamics with Monte Carlo Transport. *Astrophys. J.* **2015**, *807*, 31.
23. Ryan, B.R.; Ressler, S.M.; Dolence, J.C.; Tchekhovskoy, A.; Gammie, C.F.; Quataert, E. The Radiative Efficiency and Spectra of Slowly Accreting Black Holes from Two-Temperature GRRMHD Simulations. *ArXiv* **2017**, arXiv:1707.04238.
24. Fishbone, L.G.; Moncrief, V. Relativistic fluid disks in orbit around Kerr black holes. *Astrophys. J.* **1976**, *207*, 962–976.
25. Blandford, R.D.; Znajek, R.L. Electromagnetic extraction of energy from Kerr black holes. *Mon. Not. R. Astron. Soc.* **1977**, *179*, 433–456.
26. Blandford, R.D.; Payne, D.G. Hydromagnetic flows from accretion discs and the production of radio jets. *Mon. Not. R. Astron. Soc.* **1982**, *199*, 883–903.
27. Sądowski, A.; Narayan, R.; Penna, R.; Zhu, Y. Energy, momentum and mass outflows and feedback from thick accret ion discs around rotating black holes. *Mon. Not. R. Astron. Soc.* **2013**, *436*, 3856–3874.
28. Tchekhovskoy, A.; Narayan, R.; McKinney, J.C. Efficient generation of jets from magnetically arrested accretion on a rapidly spinning black hole. *Mon. Not. R. Astron. Soc.* **2011**, *418*, L79–L83.
29. Howes, G.G. A prescription for the turbulent heating of astrophysical plasmas. *Mon. Not. R. Astron. Soc.* **2010**, *409*, L104–L108.
30. Ressler, S.M.; Tchekhovskoy, A.; Quataert, E.; Chandra, M.; Gammie, C.F. Electron thermodynamics in GRMHD simulations of low-luminosity black hole accretion. *Mon. Not. R. Astron. Soc.* **2015**, *454*, 1848–1870.
31. Mościbrodzka, M.; Falcke, H.; Noble, S. Scale-invariant radio jets and varying black hole spin. *Astron. Astrophys.* **2016**, *596*, A13–A22.
32. Broderick, A.; Blandford, R. Covariant magnetoionic theory - II. Radiative transfer. *Mon. Not. R. Astron. Soc.* **2004**, *349*, 994–1008.
33. Dexter, J. A public code for general relativistic, polarised radiative transfer around spinning black holes. *Mon. Not. R. Astron. Soc.* **2016**, *462*, 115–136.
34. Mościbrodzka, M.; Gammie, C. ipole–Semianalytic scheme for relativistic polarized radiative transfer. *Mon. Not. R. Astron. Soc.* **2017**, in prepartion.
35. Doeleman, S.S.; Fish, V.L.; Schenck, D.E.; Beaudoin, C.; Blundell, R.; Bower, G.C.; Broderick, A.E.; Chamberlin, R.; Freund, R.; Friberg, P.; et al. Jet-Launching Structure Resolved Near the Supermassive Black Hole in M87. *Science* **2012**, *338*, 355–358.
36. Kuo, C.Y.; Asada, K.; Rao, R.; Nakamura, M.; Algaba, J.C.; Liu, H.B.; Inoue, M.; Koch, P.M.; Ho, P.T.P.; Matsushita, S.; et al. Measuring Mass Accretion Rate onto the Supermassive Black Hole in M87 Using Faraday Rotation Measure with the Submillimeter Array. *Astrophys. J. Lett.* **2014**, *783*, L33.
37. Hada, K.; Kino, M.; Doi, A.; Nagai, H.; Honma, M.; Akiyama, K.; Tazaki, F.; Lico, R.; Giroletti, M.; Giovannini, G.; et al. High-sensitivity 86 GHz (3.5 mm) VLBI Observations of M87: Deep Imaging of the Jet Base at a Resolution of 1 0 Schwarzschild Radii. *Astrophys. J.* **2016**, *817*, 131.
38. Pandya, A.; Zhang, Z.; Chandra, M.; Gammie, C.F. Polarized Synchrotron Emissivities and Absorptivities for Relativistic Thermal, Power-law, and Kappa Distrib ution Functions. *Astrophys. J.* **2016**, *822*, 34.
39. Hada, K.; Kino, M.; Doi, A.; Nagai, H.; Honma, M.; Hagiwara, Y.; Giroletti, M.; Giovannini, G.; Kawaguchi, N. The Innermost Collimation Structure of the M87 Jet Down to ˜10 Schwarzschild Radii. *Astrophys. J.* **2013**, *775*, 70.
40. Bower, G.C.; Wright, M.C.H.; Falcke, H.; Backer, D.C. Interferometric Detection of Linear Polarization from Sagittarius A* at 230 GHz. *Astrophys. J.* **2003**, *588*, 331–337.
41. Marrone, D.P.; Moran, J.M.; Zhao, J.H.; Rao, R. An Unambiguous Detection of Faraday Rotation in Sagittarius A*. *Astrophys. J. Lett.* **2007**, *654*, L57–L60.

42. Plambeck, R.L.; Bower, G.C.; Rao, R.; Marrone, D.P.; Jorstad, S.G.; Marscher, A.P.; Doeleman, S.S.; Fish, V.L.; Johnson, M.D. Probing the Parsec-scale Accretion Flow of 3C 84 with Millimeter Wavelength Polarimetry. *Astrophys. J.* **2014**, *797*, 66.
43. Martí-Vidal, I.; Muller, S.; Vlemmings, W.; Horellou, C.; Aalto, S. A strong magnetic field in the jet base of a supermassive black hole. *Science* **2015**, *348*, 311–314.
44. Liu, H.B.; Wright, M.C.H.; Zhao, J.H.; Brinkerink, C.D.; Ho, P.T.P.; Mills, E.A.C.; Martín, S.; Falcke, H.; Matsushita, S.; Martí-Vidal, I. Linearly polarized millimeter and submillimeter continuum emission of Sgr A* constrained by ALMA. *Astron. Astrophys.* **2016**, *593*, A107–A117.
45. Narayan, R.; Mahadevan, R.; Grindlay, J.E.; Popham, R.G.; Gammie, C. Advection-dominated accretion model of Sagittarius A*: Evidence for a black hole at the Galactic center. *Astrophys. J.* **1998**, *492*, 554–568.
46. Marrone, D.P. Submillimeter Properties of Sagittarius A*: The Polarization and Spectrum from 230 to 690 GHz and the Submil Limeter Array Polarimeter. Ph.D. Thesis, Harvard University, Cambridge, MA, USA, 2006.
47. Li, Y.P.; Yuan, F.; Xie, F.G. Exploring the accretion model of M87 and 3C 84 with the Faraday rotation measure observations. *ArXiv* **2016**, arXiv:1606.06029.
48. Doeleman, S.S.; Weintroub, J.; Rogers, A.E.E.; Plambeck, R.; Freund, R.; Tilanus, R.P.J.; Friberg, P.; Ziurys, L.M.; Moran, J.M.; Corey, B.; et al. Event-horizon-scale structure in the supermassive black hole candidate at the Galactic Centre. *Nature* **2008**, *455*, 78–80.